The Effect of Instantaneous Noise Injection on the Behavior of Dissipative Kerr Solitons in a Fiber Kerr Resonator

Zhiqiang Wang and Zuxing Zhang

***Abstract*—We numerically investigated the behavior of dissipative Kerr solitons (DKSs) in fiber Kerr resonators when random noise fields are suddenly applied to the system. Simulation results based on an iterative computation of an Ikeda-map-like equation system show the first observation of the annihilation and excitation of DKS under the stimulation of the noise with different intensities. Switching among different states of DKSs triggered by high amplitude noise is observed. These results have confirmed the robustness of DKSs against noise perturbations and provide new insights into the DKS dynamics in Kerr resonators, thus opening a new way to achieve different DKS states in fiber Kerr resonators.**

***Index Terms*—Fiber Kerr resonators, dissipative Kerr soliton.**

I. Introduction

DISSIPATIVE Kerr solitons (DKSs) refer specifically to as the localized structures in Kerr resonators. DKSs in the time domain are coherent ultrashort pulses, and in the frequency domain are frequency combs with equidistant space distributed in the cavity [1]. The temporal DKS has been reported by Leo et al. in 2010, demonstrating the excitation of coherent temporal DKSs in a passive fiber Kerr cavity with the help of using writing pulses [1]. The DKS has a typical $sech^2$-liked broad spectrum with ultrashort pulse duration and can be excited and manipulated independently. Soon after that, T. Herr et al. demonstrated the observation of DKSs in a high-Q MgF_2 microresonator via a detuning-scan technique [2]. The DKSs in micro resonators are now popularly known as micro frequency combs and the realization of DKSs in microresonators paves the route to realizing compact on-chip femtosecond comb sources, hence fully releasing the potential of DKSs for a wide range of applications ranging from optical communications, optical metrology, spectroscopy to low noise microwave photonics [3], [4].

In coherent driven Kerr resonators, the formation of DKS is a result of the cascaded four-wave-mixing (FWM) under certain conditions of driven power and detuning [5]. Due to the parametric nature of the FWM process, phase matching is crucial for the generation of DKS. Thus, the detuning that is defined as the phase detuning of the intracavity field to the closet cavity resonance is important and serves as a control parameter to achieve different localized patterns, such as Turing pattern, breathing solitons, and DKSs, in Kerr resonators. The DKS state is found in a frequency red-detuned region where the frequency of the pump is lower than the center frequency of the resonance. However, the bistable Kerr system is unstable in the red-detuned region due to the thermal effects that cause a tilt of the resonance frequency towards lower frequencies [2], [6]. To overcome the thermal effects, various approaches including the forward and backward detuning scan [7], power-kicking [8], self-injection locking [9], and auxiliary-laser-based thermal controlling method [10] have been proposed to access the stable operation regime of DKSs in microresonators made of different materials.

In contrast to the microresonators in which the state of DKS is spontaneously formed via laser frequency scan, the formation of DKSs in fiber Kerr resonators is challenging, although the same mean equation – Lugiato-Lefever equation (LLE) – describes well the evolution of the light field in both Kerr micro resonators and passive fiber resonators [11]. The excitation of DKSs in fiber Kerr resonators is usually achieved via suitably perturbing the system [12], [13]. Although several approaches including using writing pulses to introduce the cross-phase modulation (XPM) effect between the writing pulse and intracavity field in the cavity [1], and direct amplitude or phase modulation of the pump laser [14], [15], [16], [17], [18], [19], [20] have been proposed to get DKSs in fiber Kerr resonators, these methods increase the system complexity. Simulation based on LLE reveals the spontaneous emergence of DKS via a chain of different solutions as the cavity detuning scans. However, the experimental observation of the spontaneous creation and annihilation of DKSs in fiber Kerr resonators using the detuning scan method had been reported until 2015 [21]. The drawback of this method is that the number and the temporal location of the excited DKSs are uncontrollable. An alternative way to realize the spontaneous generation

Manuscript received 29 May 2022; revised 18 August 2022; accepted 1 September 2022. Date of publication 5 September 2022; date of current version 29 September 2022. This work was supported in part by the National Nature Science Foundation of China under Grants 91950105 and 62175116, in part by the European Commission Marie Curie Individual Fellowship under Grant 891017, in part by the Jiangsu Shuangchuang Outstanding Doctor Talents Support Program under Grant CZ1060619002, and in part by the Natural Science Foundation of Jiangsu Province under Grant BK20180742. *(Corresponding author: Zhiqiang Wang.)*

Zhiqiang Wang is with the Information Materials and Intelligent Sensing Laboratory of Anhui Province, Anhui University, Hefei 230039, China, and also with the Department of Photonics, Aston University, Birmingham B4 7ET, U.K. (e-mail: ewangzhiqiang1987@hotmail.com).

Zuxing Zhang is with the Advanced Photonic Technology Lab, Nanjing University of Posts and Telecommunications, Nanjing 210023, China (e-mail: zxzhang@njupt.edu.cn).

Digital Object Identifier 10.1109/JPHOT.2022.3204208

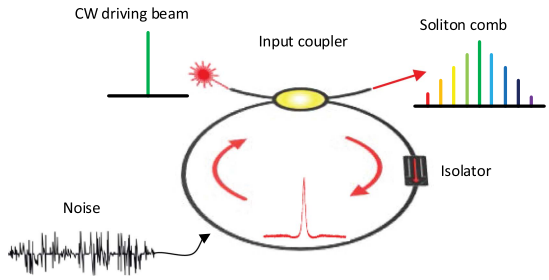

Fig. 1. Schematic of the simulation model of a fiber Kerr resonator driven by a continuous wave. Random noise is injected into the cavity only once at a selected time.

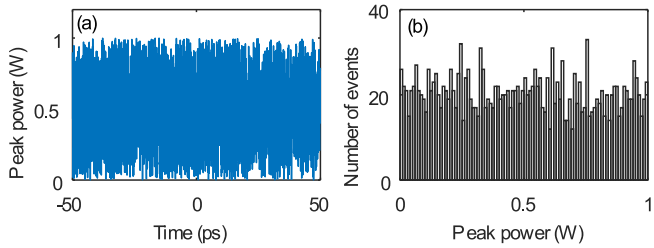

Fig. 2. Noise characteristic with maximum peak power of 1 W. (a) noise field intensity. (b) histogram bar char of the noise, showing the uniform distribution of the noise peak power in the interval of (0, 1).

of DKSs in fiber resonators is to mechanically perturb the system once the cavity detuning is locked to the cavity resonance and located in a region where the system is bistable [22]. However, detailed dynamics of DKSs under the external perturbations are lacking. Recent numerically works in [23], [24] demonstrate the deterministic generation of single DKS state in microresonators with loss modulations. The DKS has good robustness against noise perturbations in such cavities. It is hence worthy to study how the DKS responds to the noise perturbations in fiber Kerr resonators.

In this letter, we numerically studied the behavior of DKS in fiber Kerr resonators with instantaneous noise injection. Different dynamics of DKS have been observed. Under weak intensity perturbation, the precursor of DKS is annihilated, and no DKS state can be formed based on the noise field. In strong contrast, a strong noise can trigger the switching among different DKS states. Our results show that the noise perturbation can be used as one degree of freedom to control the DKS in fiber Kerr resonators.

II. Simulation Model and Principle

Although DKSs in both microresonator or fiber-based macro resonators can be well described by the LLE equation, the fiber-based system is more close to a lumped model due to the existing optical components such as optical couplers and isolators in the cavity, so that a simulation model of a standard nonlinear Schrödinger equation (NLSE) with proper boundary conditions is more suitable for simulations of fiber resonators, especially in a tristable passive Kerr cavity in which the resonance curve are overlapped with one another due to the resonance tilt [17]. A schematic of our simulation model is depicted in Fig. 1. The resonator is a fiber cavity consisting of a loop of 108 meters of single-mode fiber (SMF) with a group velocity dispersion (GVD) of -22 ps^2/km and nonlinearity coefficient of 1.2 W^{-1}/km at 1550 nm, respectively. The total cavity loss is 22%. The cavity roundtrip time is 524 ns, which is determined by the total cavity length, thus yielding a pulse repetition rate of 1.91 MHz.

The pulse propagating in SMF is governed by the NLSE concerning the effects of dispersion, nonlinearity as well as loss.

$$\frac{\partial E_m(z,t)}{\partial z} = -\frac{\alpha}{2}E_m - i\frac{\beta_2}{2}\frac{\partial E_m}{\partial t} + i\gamma|E_m|^2 E_m \quad (1)$$

where E_m is the intracavity field. α represents the total cavity loss. β_2 is the fiber group velocity dispersion (GVD) and γ denotes the fiber nonlinearity coefficient. High-order effects such as higher-order dispersion, self-steepening, and the Raman effect have been neglected without loss of the generality of our simulation results.

The boundary condition at a roundtrip m is given by.

$$E_{m+1}\ (z\ =\ 0,t) = \sqrt{\theta}\ E_{in} + \sqrt{\rho}E_m\ (z\ =\ L,t)\ e^{-i\delta} \quad (2)$$

Where E_{m+1} is the light field at $m+1$ roundtrip. E_{in} is the CW-driven field, θ is the input coupling coefficient of the coupler located at $z\ =\ 0$, and δ is the phase detuning describing the frequency shift between the driven field and cavity resonance frequency. The focus of this paper is to investigate the behavior of DKS affected by the transient noise, therefore, we inject a random noise field E_{noise} with peak power varying from 0 to P_{max} into the cavity only once at a selected detuning δ when there are stable DKSs formed in the cavity. In simulations, the noise is generated by using a built-in $rand(n)$ function in MATLAB.

$$E_{noise}\ (t) = P_{noise} * \text{rand}\ \ (n) \quad (3)$$

Where $rand$ function creates a 1-by-n array of random numbers, which is uniformly distributed in the interval of $(0, 1)$. P_{noise} determines the maximum peak power of the noise. Fig. 2(a) shows a noise with maximum peak power of 1 W and (b) is the histogram bar chart of the noise intensity over the fast time window of 100 ps. We emphasize that other noise, such as a random noise with standard normal distribution, can also be used for our simulation, but the resulting DKS dynamics in these two different situations are similar. Therefore, in the following study, we only used uniformly distributed random noises as a typical representative, without losing the generality of the dynamics.

The noise is added onto the intracavity field at a time when the intracavity field converges into a steady state of DKS at a certain detuning δ_{fixed}.

$$E_{m+1}\ (z,t)\ = E_m\ \ (z,t) + E_{noise}\ (t) \quad (4)$$

After the noise injection, the intracavity field will continue propagating in the cavity for hundreds of roundtrips with the fixed detuning δ_{fixed}.

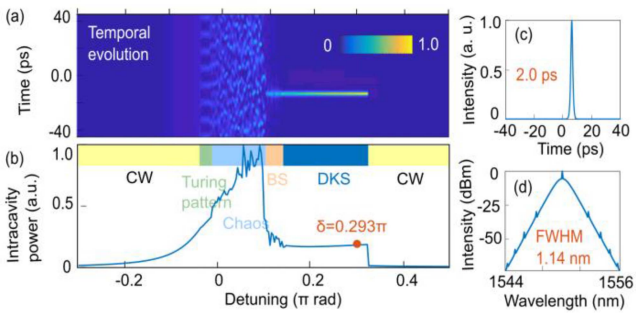

Fig. 3. Simulation results of the Ikeda map of the intracavity dynamics during detuning scan. (a) intracavity field evolution in the time domain. (b) the corresponding intracavity power evolution. The different color region shown on the top indicates the different detuning region for different operating regimes. (c) Pulse profile and (d) spectrum profile corresponding to the DKS at a detuning of 0. 293π marked with an orange dot in (b).

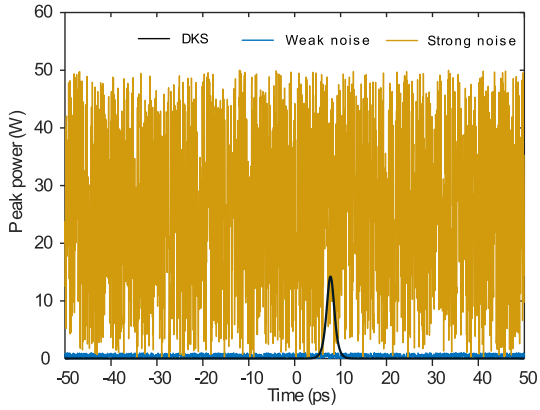

Fig. 4. The intensity distribution of weak noise and strong noise, respectively. The pulse intensity profile of a single DKS is also given for comparison.

III. Simulation Results

A. Ikeda Map Confirming the DKS Generation

We performed simulations of the intracavity field evolution at a constant pump power of 0.5 W via linearly scanning the detuning from a blue-detuned into a red-detuned region, aiming to first confirm the existence of DKS in the proposed system. For each detuning, we run 1000 roundtrips to make sure that the intracavity field converges to a steady-state solution at the end. Then the obtained solution is used as the initial condition for the next detuning value.

In the process of detuning scanning, different operation regimes have been observed. Fig. 3(a) depicts the evolution of the intracavity field in the time domain as detuning scans. Five distinct regimes are formed in different detuning ranges, following a chain continues wave (CW), stable MI pattern, chaos, breathing DKS, and stable DKS. The observed dynamics in the chain in our simulations are well consistent with the theoretical and experimental observations in other reports, confirming the validity of our model [25], [26], [27]. Fig. 3(c) depicts the intracavity power evolution, showing explicitly parameter boundaries for different operating regimes. The orange dot is marked at $\delta = 0.293\pi$ and the corresponding pulse profile and the spectrum is shown in Fig. 3(c) and (d), as an example of the DKS, respectively, confirming the generation of a 2 ps single DKS with a full width at half maximum (FWHM) of 1.14 nm. The pulse energy is 35 pJ. The narrow peak located in the center of the spectrum is the residual CW pump and the weak Kelly-like sidebands appearing atop the CS spectrum are because of the periodic cavity loss perturbations in every roundtrip [28].

B. Dynamics of Single DKS Under Instantaneous Noise Injection

To study the impact of the instantaneous noise injection on DKS behavior, we carried out simulations by suddenly adding a noise field onto the intracavity field at a time when stable DKS is formed in the cavity. Specifically, we first scan the detuning from an initial value of $\delta = -0.5\pi$ to $\delta = 0.293\pi$ in the first 250 roundtrips, getting stable DKS state and subsequently inject the noise into the cavity once and keep $\delta_{fixed} = 0.293\pi$ for running simulation in the further hundreds of roundtrips. Next, we consider the behavior of DKSs in conditions of instantaneous noise injection with different intensities. In our simulations, the definition of the noise as a weak or a strong one is based on the ratio between the maximum peak power (P_{max}) of the noise and the intracavity power. Another criterion is to compare the maximum peak power of the noise to the threshold of the modulation instability (MI) in optical fibers under the condition of anomalous dispersion ($\beta_2 < 0$). A corrected empirical threshold of MI in optical fiber can be expressed as [29]:

$$P_{crit}^{MI} = 5/2\gamma L_{eff} \tag{5}$$

where L_{eff} is the effective fiber length. Considering the fiber cavity length of 108 m in our case, the estimated MI threshold is 19.3 W. The peak power of DKS $at\ \delta = 0.293\pi$ is about 14 W. Therefore, for the weak noise case, we set P_{max} to be only 1 W, which is much lower than the peak power of DKS and also the MI threshold value, whereas the strong noise field has a $P_{max} = 50\ W$, which is higher than P_{crit}^{MI} and almost 3.5 times the peak power of DKS. Fig. 4 depicts the intensity distribution of the weak noise (Cyan curve) and the strong noise (yellow curve), respectively, and the pulse intensity of a single DKS (black curve) is also shown in Fig. 4 as a comparison.

For comparison, we first show in Fig. 5(a) the simulation results of the Ikeda map without noise injection. The horizontal dashed white line cuts at $\delta_{fixed} = 0.293\pi$. Without noise perturbation, the DKS is seen to evolve with maintaining its shape. Once the system is disturbed, as we expect, the DKS state is changed. Fig. 5(b) shows the dynamics of the annihilation of a single DKS caused by the weak perturbations to the system. The inset is the zoom-in of the DKS annihilation process. While under strong perturbations, two different scenarios have been observed: one is that a new DKS is excited to accompany the annihilation of the preexisting DKS (Fig. 5(c)) and the other is that a single DKS state transforms into a new state of two DKSs (Fig. 5(d)). The evolution of the intracavity power shown in Fig. 6 shows clear evidence of the annihilation and excitation of DKSs in the noise perturbation process.

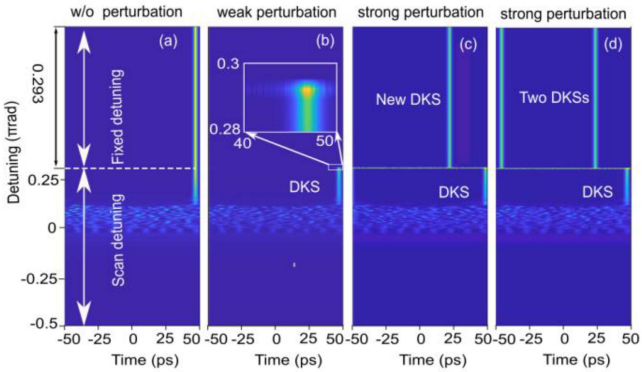

Fig. 5. Simulation of the intracavity dynamics caused by instantaneous noise injection. The detuning is continuously scanning from an initial value of -0.5π to 0.293π and then remains constant at 0.293π for further roundtrips. Ikeda map without perturbations (a), with weak perturbations (b), and with strong perturbations (c and d). The inset in the white rectangular box in (b) is an enlarged view of the dynamics in the small white box, highlighting the weak perturbations.

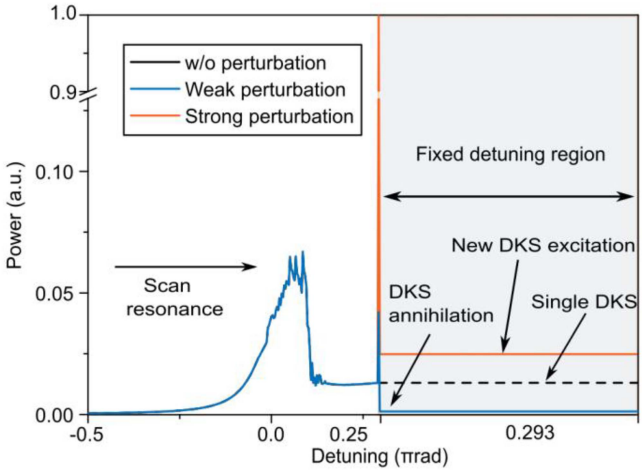

Fig. 6. Intracavity power evolution, corresponding to the dynamics shown in Fig. 5(a) (Black dotted line), (b) (blue line), and (d) (red line), respectively. The power is normalized to the maximum peak power of the noise perturbations.

C. Dynamics of Multi-DKSs Under Instantaneous Noise Injection

Using random noise as initial conditions to simulate the Ikeda map, the pattern of the spontaneous excited DKSs could be different. On the other hand, without external control, the usual observed DKS states in fiber Kerr resonators are always multi-DKSs. Therefore, it is of interest to investigate how the noise perturbation affects the behavior of multi-DKSs in fiber Kerr resonators. For simplicity, without loss of generality, we limited our simulation to the case of only two DKSs and studied the perturbation-induced dynamics (Fig. 6). It's natural to see that without instantaneous perturbations the preformed two DKSs in the process of scanning detuning from $\delta = -0.5\pi$ to $\delta = 0.293\pi$ can be sustained in the following fixed detuning scan process. When the noise is suddenly injected to perturb the system, in addition to the observation of the annihilation of DKSs caused by the weak perturbation (Fig. 7(b)), we also see

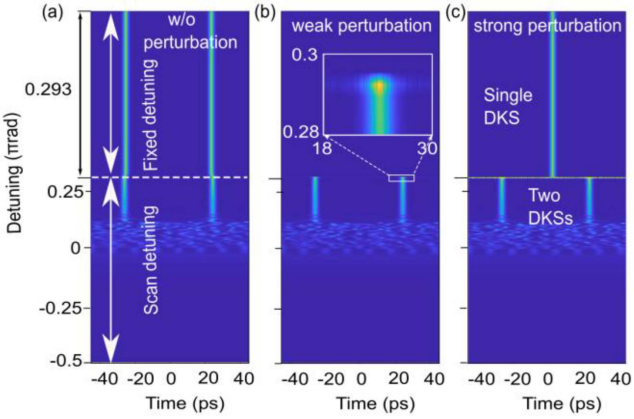

Fig. 7. Simulation of the intracavity dynamics of two DKSs caused by instantaneous noise injection. Ikeda map without perturbations (a), with weak perturbations (b), and with strong perturbations (c). The inset in the white rectangular box in (b) is an enlarged view of the dynamics in the small white box, highlighting the weak perturbations.

switching from a two DKSs state to a single DKS state under the condition of strong noise injection (Fig. 7(c)). These results indicate the universality of using the method of instantaneous noise injection to control the DKS states in Kerr resonators.

D. Dynamics of the DKS Annihilation and Excitation

To figure out the mechanisms of the noise-injection induced annihilation and excitation of DKS, we dissected the dynamics of the evolution of a stable DKS with instantaneously noise injection. When the pump power is 0.5 W and the detuning is $\delta = 0.293\pi$, the steady state in the cavity is stable single DKS. We use the stable single DKS as the initial condition for the following simulations. The pump power and the detuning are constant. A random noise with a peak power of 1 W is added onto the intracavity field at the roundtrip (RT) of 50 once. Fig. 8(a) depicts the evolution of the temporal pulse profile and Fig. 8(b) is an enlarged version of the dynamics within the range from RT 40 to 70, showing that the sudden injected noise destroyed the DKS states. No MI occurs because of the low peak power of the noise field. The corresponding evolution of the spectrum is shown in Fig. 8(c), further confirming the lack of the MI pattern. It is well known that the Kerr system is sensitive to initial conditions. Therefore, no DKS is formed after the noise perturbations as of the improper initial conditions. The spectrum at RT 130 shown in Fig. 8(d1) is the final state of CW operation.

In strong contrast, under the sudden perturbation of strong noises, the noticeable difference is the emergence of the MI pattern after the noise injection, which is evidenced by the temporal chaotic pattern and the unsmooth broad spectrum shown in Fig. 9(b2) and (d2), respectively. Although no stable MI pattern of Turing pattern is formed at this detuning, the MI-induced chaotic pulses are randomly distributed within the whole cavity (see Fig. 9(b2)), and thus new DKSs can be formed based on these MI-induced pulses as initial conditions. A temporal shift of the location of the DKS shown in Fig. 9(b1) confirms the formation of new DKS. Besides, the MI patterns are partially

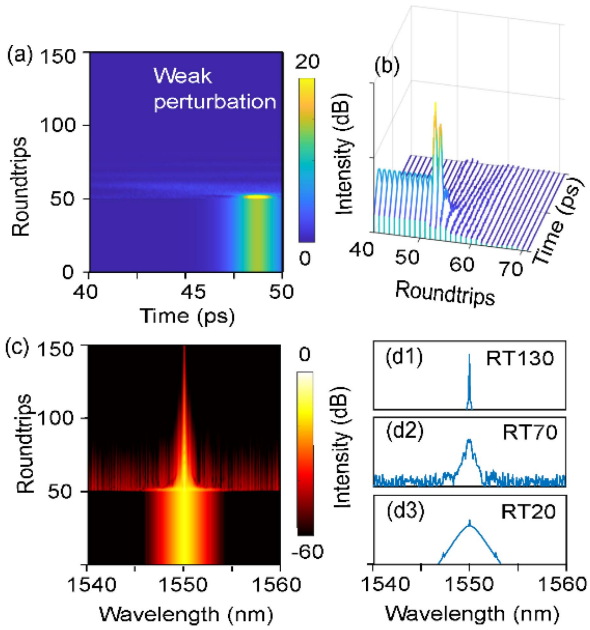

Fig. 8. Simulation results of the dynamics of DKSs under weak perturbations as a function of roundtrips. The pump power is 0.5 W and the detuning δ is 0.293π rad. (a) Temporal profile evolution. (b) Waterfall of pulse evolution from RT 40 to 70. (c). Spectral profile evolution. (d) the spectrum at the RT 20, RT 70, and RT 130, respectively.

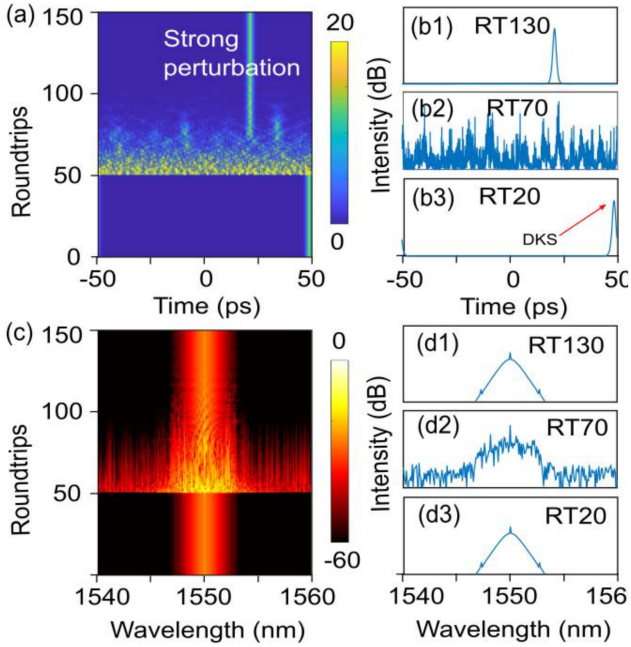

Fig. 9. Simulation results of the dynamics of DKSs under strong perturbations as a function of roundtrips (RT). The pump power is 0.5 W and the detuning δ is 0.293π rad. (a) Temporal profile evolution. (b) the spectrum at the RT 20, RT 70, and RT 130, respectively. (c) Spectral profile evolution. (d) the spectrum at the RT 20, RT 70, and RT 130, respectively.

coherent states with localized spectrum in the frequency domain (Fig. 9(d2)), which are similar to the chaotic states that emerge on the route towards the DKS state when scanning the detuning from the blue-detuned region to the red-detuned region crossing the resonance peak. Therefore, we attribute the excitation of the new DKS to the MI that takes place under strong noise perturbations.

E. Discussion

We remind ourselves that the peak power of the noise field used in the simulations is at the Watt level, specifically in a range from a few Watts to up to 50 W. Therefore, an ASE source that is amplified by an EDFA could generate the desired noise before the injection into the cavity in practical. Another practical solution to create a random noise with such a high peak power is using incoherent chaotic pulse structures such as pulse bunch or noise-like pulses (NLP) [30], [31]. NLP is the temporally localized structure composed of multiple soliton-like pulses that differ in their amplitudes lacking mutual phase coherence and hence move at different speeds and interact with each other, leading to the generation of extreme waves. Therefore, the NLP from a partially mode-locked laser source could yield the desired noise. Since the noise is only added into the cavity once, the offset between the repetition rate of the NLP and the cavity roundtrip time is not a problem.

Our simulation results provide decisive evidence that the DKSs can be excited in Kerr resonators under the stimulation of instantaneous noise injection. Such an instantaneous noise perturbation can drive the system out of equilibrium, enabling the spontaneous generation of DKSs in Kerr fiber resonators. The formed pattern is dependent on the perturbation strength. In our simulations, a weak perturbation usually destroys the stable DKS state, while a strong one enables the excitation of MI patterns, leading to the formation of DKSs eventually. A simple analysis of the MI threshold in optical fiber and the simulation results reveal the critical value of the intensity of noise that dominates the DKSs behaviors.

Let's remind that in the precondition of locking the pump frequency to the cavity resonance, using the detuning scan method, the spontaneous generation of DKS in fiber Kerr resonators is still challenging. The excitation of DKS in fiber Kerr resonators requires firstly the lock of the pump frequency to a proper position with respect to the cavity resonant frequency and second, and more importantly, external perturbations. One may notice that the onset of the DKS state in the detuning scan process in Kerr resonators is usually accompanied by a sudden drop in the intracavity power. The drastic power drop could manifest as noise emission in the cavity that could be used for DKS generation in fiber Kerr resonators via using our proposed approach – instantaneous noise injection. This inspires us to come up with a simple one-step detuning lock for exciting DKS in fiber Kerr resonators: a sudden lock of the detuning could realize the excitation of DKS states in fiber Kerr resonators without external perturbations, hence greatly simplifying the system setup. Indeed, we achieved multiple stable DKS states via our proposed one-step detuning lock method experimentally and the relative mechanism is being studied. We expect to present the related results elsewhere soon.

Furthermore, the fiber resonator has the flexibility to generate DKS at a pulse repetition rate of kHz or MHz, much lower

than hundreds of GHz or even up to THz in microresonators, real-time techniques like dispersion Fourier transform [32] or time lens [33] can be used to full-field characterize the DKS buildup dynamics and also the noise-induced annihilation or excitation transient dynamics in real-time, which will deepen our understanding of DKSs in Kerr resonators.

V. Conclusion

To conclude, we have numerically shown that different DKS states can be obtained in a CW-driven fiber Kerr resonates under instantaneous noise perturbations. The strength of the noise perturbation can impact the excited CS patterns. The annihilation, excitation, and switching of DKS states under the perturbation of noise are observed. The feasibility of experimental schemes is also discussed. Our results pave the way to use the noise perturbation to get access to the DKS regime and to control the DKS behavior in Kerr resonators. These findings improve our understanding of the dynamics of DKS and may impact the design of robust soliton comb sources.

References

[1] F. Leo, S. Coen, P. Kockaert, S.-P. Gorza, P. Emplit, and M. Haelterman, "Temporal cavity solitons in one-dimensional Kerr media as bits in an all-optical buffer," *Nature Photon.*, vol. 4, pp. 471–476, 2010.

[2] T. Herr et al., "Temporal solitons in optical microresonators," *Nature Photon.*, vol. 8, pp. 145–152, 2014.

[3] P. Del'Haye, A. Schliesser, O. Arcizet, T. Wilken, R. Holzwarth, and T. Kippenberg, "Optical frequency comb generation from a monolithic microresonator," *Nature*, vol. 450, pp. 1214–1217, 2007.

[4] P. Trocha et al., "Ultrafast optical ranging using microresonator soliton frequency combs," *Science*, vol. 359, pp. 887–891, 2018.

[5] T. Kippenberg, R. Holzwarth, and S. Diddams, "Microresonator-based optical frequency combs," *Science*, vol. 332, pp. 555–559, 2011.

[6] T. Carmon, L. Yang, and K. J. Vahala, "Dynamical thermal behavior and thermal self-stability of microcavities," *Opt. Exp.*, vol. 12, pp. 4742–4750, 2004.

[7] H. Guo et al., "Universal dynamics and deterministic switching of dissipative Kerr solitons in optical microresonators," *Nature Phys.*, vol. 13, pp. 94–102, 2017.

[8] V. Brasch et al., "Photonic chip–based optical frequency comb using soliton Cherenkov radiation," *Science*, vol. 351, pp. 357–360, 2016.

[9] N. Pavlov et al., "Narrow-linewidth lasing and soliton Kerr microcombs with ordinary laser diodes," *Nature Photon.*, vol. 12, pp. 694–698, 2018.

[10] H. Zhou et al., "Soliton bursts and deterministic dissipative Kerr soliton generation in auxiliary-assisted microcavities," *Light: Sci. Appl.*, vol. 8, pp. 1–10, 2019.

[11] L. Lugiato, F. Prati, M. Gorodetsky, and T. Kippenberg, "From the Lugiato–Lefever equation to microresonator-based soliton Kerr frequency combs," *Philos. Trans. Roy. Soc. A: Math., Phys. Eng. Sci.*, vol. 376, 2018, Art. no. 20180113.

[12] F. Hopf, P. Meystre, P. Drummond, and D. Walls, "Anomalous switching in dispersive optical bistability," *Opt. Commun.*, vol. 31, pp. 245–250, 1979.

[13] M. Haelterman, S. Trillo, and S. Wabnitz, "Dissipative modulation instability in a nonlinear dispersive ring cavity," *Opt. Commun.*, vol. 91, pp. 401–407, 1992.

[14] Y. Wang, B. Garbin, F. Leo, S. Coen, M. Erkintalo, and S. G. Murdoch, "Addressing temporal Kerr cavity solitons with a single pulse of intensity modulation," *Opt. Lett.*, vol. 43, pp. 3192–3195, 2018.

[15] I. Hendry et al., "Spontaneous symmetry breaking and trapping of temporal Kerr cavity solitons by pulsed or amplitude-modulated driving fields," *Phys. Rev. A*, vol. 97, 2018, Art. no. 053834.

[16] M. Anderson, F. Leo, S. Coen, M. Erkintalo, and S. G. Murdoch, "Observations of spatiotemporal instabilities of temporal cavity solitons," *Optica*, vol. 3, pp. 1071–1074, 2016.

[17] M. Anderson, Y. Wang, F. Leo, S. Coen, M. Erkintalo, and S. G. Murdoch, "Coexistence of multiple nonlinear states in a tristable passive Kerr resonator," *Phys. Rev. X*, vol. 7, 2017, Art. no. 031031.

[18] G. Xu et al., "Spontaneous symmetry breaking of dissipative optical solitons in a two-component Kerr resonator," *Nature Commun.*, vol. 12, pp. 1–9, 2021.

[19] J. K. Jang, M. Erkintalo, S. G. Murdoch, and S. Coen, "Writing and erasing of temporal cavity solitons by direct phase modulation of the cavity driving field," *Opt. Lett.*, vol. 40, pp. 4755–4758, 2015.

[20] V. Lobanov, G. Lihachev, N. Pavlov, A. Cherenkov, T. Kippenberg, and M. Gorodetsky, "Harmonization of chaos into a soliton in Kerr frequency combs," *Opt. Exp.*, vol. 24, pp. 27382–27394, 2016.

[21] K. Luo, J. K. Jang, S. Coen, S. G. Murdoch, and M. Erkintalo, "Spontaneous creation and annihilation of temporal cavity solitons in a coherently driven passive fiber resonator," *Opt. Lett.*, vol. 40, pp. 3735–3738, 2015.

[22] Z. Li, Y. Xu, S. Coen, S. G. Murdoch, and M. Erkintalo, "Experimental observations of bright dissipative cavity solitons and their collapsed snaking in a Kerr resonator with normal dispersion driving," *Optica*, vol. 7, pp. 1195–1203, 2020.

[23] Z. Xiao, K. Wu, T. Li, and J. Chen, "Deterministic single-soliton generation in a graphene-FP microresonator," *Opt. Exp.*, vol. 28, pp. 14933–14947, 2020.

[24] Y. Chen, T. Liu, S. Sun, and H. Guo, "Temporal dissipative structures in optical Kerr resonators with transient loss fluctuation," *Opt. Exp.*, vol. 29, pp. 35776–35791, 2021.

[25] S. Coen and M. Erkintalo, "Universal scaling laws of Kerr frequency combs," *Opt. Lett.*, vol. 38, pp. 1790–1792, 2013.

[26] T. J. Kippenberg, A. L. Gaeta, M. Lipson, and M. L. Gorodetsky, "Dissipative Kerr solitons in optical microresonators," *Science*, vol. 361, 2018, Art. no. eaan8083.

[27] Z. Kang et al., "Deterministic generation of single soliton Kerr frequency comb in microresonators by a single shot pulsed trigger," *Opt. Exp.*, vol. 26, pp. 18563–18577, 2018.

[28] A. U. Nielsen, B. Garbin, S. Coen, S. G. Murdoch, and M. Erkintalo, "Invited article: Emission of intense resonant radiation by dispersion-managed Kerr cavity solitons," *APL Photon.*, vol. 3, 2018, Art. no. 120804.

[29] S. M. Foaleng and L. Thévenaz, "Impact of Raman scattering and modulation instability on the performances of Brillouin sensors," in *Proc. 21st Int. Conf. Opt. Fiber Sensors*, 2011, pp. 1450–1453.

[30] C. Lecaplain, P. Grelu, J. Soto-Crespo, and N. Akhmediev, "Dissipative rogue waves generated by chaotic pulse bunching in a mode-locked laser," *Phys. Rev. Lett.*, vol. 108, 2012, Art. no. 233901.

[31] Z. Wang, K. Nithyanandan, A. Coillet, P. Tchofo-Dinda, and P. Grelu, "Buildup of incoherent dissipative solitons in ultrafast fiber lasers," *Phys. Rev. Res.*, vol. 2, 2020, Art. no. 013101.

[32] A. Mahjoubfar, D. V. Churkin, S. Barland, N. Broderick, S. K. Turitsyn, and B. Jalali, "Time stretch and its applications," *Nature Photon.*, vol. 11, pp. 341–351, 2017.

[33] P. Ryczkowski, M. Närhi, C. Billet, J.-M. Merolla, G. Genty, and J. M. Dudley, "Real-time full-field characterization of transient dissipative soliton dynamics in a mode-locked laser," *Nature Photon.*, vol. 12, pp. 221–227, 2018.